



Published in final edited form as:

*Adv Healthc Mater.* 2013 February ; 2(2): 266–270. doi:10.1002/adhm.201200148.

## An Automated Process for Layer-by-Layer Assembly of Multilayer Thin Films on Viable Cell Aggregates

**Joseph M. Mets,**

Wallace H. Coulter Department of Biomedical Engineering, Georgia Institute of Technology and Emory University School of Medicine, Atlanta, GA, 30332 (USA)

**Dr. John T. Wilson,**

Wallace H. Coulter Department of Biomedical Engineering, Georgia Institute of Technology and Emory University School of Medicine, Atlanta, GA, 30332 (USA)

**Dr. Wanxing Cui, and**

Wallace H. Coulter Department of Biomedical Engineering, Georgia Institute of Technology and Emory University School of Medicine, Atlanta, GA, 30332 (USA)

**Prof. Elliot L. Chaikof**

Department of Surgery, Beth Israel Deaconess Medical Center, Harvard Medical School, and the Wyss Institute of Biologically Inspired Engineering of Harvard University, 110 Francis Street, Suite 5B, Boston MA, 02115 (USA)

Elliot L. Chaikof: echaikof@bidmc.harvard.edu

### Abstract

**An automated process for modifying the surface of pancreatic islets** grows uniform polyelectrolyte multilayer thin films, eliminating user variability associated with previous manual methods. Machine vision feedback allows for tight control of small fluid volumes, maintaining islet microenvironment. This process is adaptable to other fragile micron-scale particle systems.

### Keywords

cell surface engineering; islet transplantation; machine vision; microparticle coating; polyelectrolyte multilayer films

---

Type 1 diabetes affects at least 30,000 new patients per year in the United States alone and is typically fatal without regular blood glucose monitoring and daily administration of exogenous insulin.<sup>[1, 2]</sup> It has long been postulated that transplantation of pancreatic islets of Langerhans into patients with Type 1 diabetes could restore glucose sensing and insulin secretion functions, eliminating the need for constant self-monitoring and insulin injection with superior control over blood glucose levels.<sup>[3, 4]</sup> However, achieving this goal remains elusive. Even with recent improvements, lifelong immunosuppression is required, often two or three separate islet transplants are generally needed to achieve euglycemia, and far fewer than half of all patients are insulin independent one year after transplantation.<sup>[5–7]</sup>

Re-engineering the biological and chemical properties of islet surfaces has recently emerged as a promising approach to improving clinical outcomes after islet transplantation. Notable

---

Correspondence to: Elliot L. Chaikof, echaikof@bidmc.harvard.edu.

Supporting Information

Supporting Information is available from the Wiley Online Library or from the author.

examples include immobilization of anti-inflammatory and anti-coagulant molecules on islet surfaces,<sup>[8–13]</sup> surface grafting of poly(ethylene glycol) as a steric barrier between the graft and the host immune system,<sup>[14–20]</sup> and deposition of cell surface-supported polymeric thin films via layer-by-layer (LbL) and other techniques as a nanoscale cell encapsulation strategy.<sup>[21–32]</sup> Our group has recently described a novel approach for cell surface engineering through the LbL self assembly of polyelectrolyte multilayer (PEM) thin films directly on the surface of pancreatic islets, as described in Figure 1.<sup>[24, 25]</sup> As a bottom-up approach to cell surface engineering, LbL films offer unprecedented versatility and modularity relative to conventional cell surface modification approaches. Significantly, LbL film properties can readily be tailored through control of film constituents, layer number, and fabrication conditions.<sup>[33–41]</sup> Moreover, diverse biological molecules and nanoscale materials can be readily integrated into LbL films, providing a highly versatile scaffold for the localized presentation and release of biologically active agents that serve to improve islet survival and engraftment.<sup>[25]</sup>

Central to LbL films' success in islet cell surface engineering was our discovery of a novel subset of poly(L-lysine)-graft-poly(ethylene glycol) (PLL-g-PEG) cationic copolymers, similar to previous grafted copolymers studied by others as single-layer coatings for cells and nonliving substrates.<sup>[42–46]</sup> Unlike most polycationic materials, PLL-g-PEG copolymers exhibit minimal cytotoxicity, while simultaneously facilitating the growth of LbL films directly on the surface of pancreatic islet cells. Films can be assembled without adversely influencing islet viability or function, loaded with a model biologic therapeutic, and resulted in improved rates of conversion to euglycemia in a murine model of islet transplantation.<sup>[24, 25]</sup> Despite this success, the assembly of LbL films on islets remains a tedious and time consuming process that required a trained technician and was subject to human variability. Manipulation of islets is difficult because they are small (50 to 200  $\mu\text{m}$ ), approximately spherical multicellular aggregates whose structural integrity and biological function are sensitive to mechanical forces, removal from culture media, and withdrawal across air-water interfaces. These effects are magnified by the repetitive solution exchanges inherent to LbL assembly, and, therefore, any strategy to apply thin film coatings to islets must account for these forces.

In our experience, aqueous microparticle coating strategies reported by others, namely centrifugation,<sup>[47]</sup> selective withdrawal,<sup>[48]</sup> and microfluidics,<sup>[49]</sup> were not amenable to LbL film assembly on islets. Centrifugation predisposes islets to mechanical damage secondary to repeated exposure to centripetal forces, pellet formation, and pellet dispersion. Selective withdrawal is not easily compatible with the high number of washes and incubations that LbL film assembly requires. Microfluidics approaches would be limited by scalability; a prohibitively large number of units would be necessary in order to process suitable numbers of islets in a timely fashion. Previously, our group has employed a manual filtration technique where islets were placed in standing cell culture inserts (Millipore, Billerica, Massachusetts) that facilitated the drainage of polyelectrolyte and wash solutions while retaining islets.<sup>[24, 25]</sup> Solutions were injected by hand pipette and evacuated through microporous mesh on the inferior surface by manually tapping the insert repeatedly on a sterile polystyrene surface, which facilitated drainage of solution through capillary forces. When performed correctly by experienced hands, manual filtration was successful in producing islets encapsulated in LbL films that were fully functional and highly viable. However, the technique was limited by the inability to precisely regulate fluid levels in the insert during evacuation. Over-evacuation would expose islets to air-water interfaces, causing damage. Under-evacuation would result in deviation of polymer concentrations from the tight ranges compatible with PEM film growth. Furthermore, manual filtration was especially demanding of skilled technicians' time, a valuable resource in the modern

laboratory setting. All of these factors would limit the potential to scale this process from a laboratory environment to a more relevant clinical setting.

Herein, we describe an automated filtration process for assembly of LbL films on pancreatic islets. To achieve this, we employed novel machine-vision technology to allow for exquisite regulation of reactor volumes, polyelectrolyte concentrations, incubation times, and flow rates. This process reduced the potential for user variability, increased efficiency, and eliminated the laborious aspects of our previous approach, while retaining the design aspects that contributed to the success of manual filtration (Table 1). Significantly, this process has a broad array of potential applications in areas such as drug delivery and cell surface engineering, and is readily amenable to automated coating of diverse micron-sized particles. Additionally, the machine vision method of precise small volume measurement has potential applications in fields ranging from chemical synthesis and biological culture to manufacturing and sensors.

Design of the automated coating apparatus was centered around sterile, disposable 0.6 mL reactors (standing cell culture inserts, 0.6 cm<sup>2</sup> filtration area, Millipore, Billerica, MA) with 12 μm microporous mesh on the inferior surface. A reactor-to-Luer Lock fitting (custom fabricated from extruded acrylic by numerically controlled milling) allowed solution withdrawal through the reactor's mesh floor. Computer controlled syringe pumps and small 10 mL syringes were chosen to precisely inject and evacuate solutions. Pinch valves (ValveBank, AutoMate Scientific, Berkeley, California) and reservoirs were incorporated to purge or refill syringes as necessary, so coating protocol length was limited only by reservoir size. A computer program was written in LabView (National Instruments, Austin, Texas) to control the process. A more detailed schematic of the custom fabricated reactor and coating system is shown in Figure S1 in Supporting Information.

We quickly found that system feedback was necessary to prevent the propagation of relatively small reactor under-evacuation or over-evacuation errors, which consistently caused reactor overflow or islet damage, respectively. A USB webcam (QuickCam 4000, Logitech, Fremont, California) was incorporated to provide machine vision (MV) fluid level measurements as seen in Figure 2 and further detailed in Figure S2 in Supporting Information. Fluid level control was assessed by loading the reactor with an arbitrary amount of islet wash buffer, evacuating briefly to form a consistently shaped meniscus, and taking a MV fluid level measurement. Then, prior to full evacuation, fluid was carefully aspirated by pipette and weighed as a benchmark measurement. A 0<sup>th</sup> order calibration factor was added to account for the small but significant amount of fluid above the bottom of the meniscus, which the MV algorithm was otherwise unable to detect. After calibration, MV measurements showed a strong correlation with weight-based measurements ( $r^2=0.995$ ,  $n=10$ ). Mean magnitude of error was 4.51 μL. For all experiments presented here, calibration factors were recalculated each time a new reactor was installed and consistently fell between 85 μL and 110 μL. In order to maximize washing efficiency and prevent the exposure of islets to air, the system was configured so that a small “void volume” of solution remained in the reactor after evacuation. Void volume was set to 60 μL, the empirically determined minimum volume at which the mesh floor would be completely covered in solution.

Having established a satisfactory method to control solution volumes in the reactor, the system's ability to process murine islets was characterized. First, process yield was determined. The LabView program was configured to execute an 8 bilayer coating protocol with three washes and two 5 minute incubation steps per bilayer. This protocol took 2.5 hours to complete and a mean of 91% islets were recoverable after 6 independent experiments (95% CI: 84% to 99%). Recovery rate was similar between experiments

performed with low numbers of islet number (21–44 islets, n=5, 91% mean recovery) and those with higher islet numbers (200 islets, n=1, 95% recovery). These investigations were performed with islet wash buffer in place of polyelectrolyte solutions to isolate the effect of mechanical forces on islet loss. Recovery rates, protocol time, and the capacity of the system to handle at least 200 islets were sufficient to assess the automated system's effects on PEM film growth.

The development of PEM films on islets is mediated through alternating deposition of polycationic and polyanionic polymers, as demonstrated previously.<sup>[25]</sup> PLL-g-PEG/alginate films were assembled on planar substrates as previously described.<sup>[25]</sup> These films were readily disassembled when immersed in 5 M sodium chloride (Figure S3), demonstrating that electrostatic interactions dominate film assembly and supporting the polyelectrolyte multilayer model of film architecture. Coating development in the automated system was assessed using PLL-g-PEG as the polycation and fluorescein-labeled alginate (F-alg) as the polyanion. Laser scanning confocal microscopy (LSCM) clearly demonstrated the presence of uniform PEM films on autocoated islets (Figure 3a). Moreover, LSCM suggested that films conformed to the geometrically and chemically heterogeneous islet surface, similar to those assembled manually.

Maintenance of islet viability and function is critical to the success of islet transplantation. To assess any impact of this process on islet viability, islets were first autocoated with 8 bilayers of polycation and polyanion without fluorescent tags. Live/dead staining with calcein AM (viable) and ethidium homodimer (nonviable) was performed and images of individual islets were obtained using LSCM. Viability for each islet, defined as viable-stained area divided by area that stained with either dye, was calculated with an image processing algorithm. Autocoated islets (n=50, 99.3% viable) were as viable as islets that were maintained in culture without manipulation (n=46, 99.3% viable, p=0.7, Figure 3b). Islets subjected to centrifugation at 3000 rpm for 15 minutes, a treatment known in our experience to induce minor but discernable damage, displayed a small but statistically significant reduction in islet viability (n=31, 97.9% viable; p=2.25 × 10<sup>-7</sup>). These data demonstrate that the autocoating process has no effect on biological viability.

Murine islets with high viability and function adopt a spherical, smooth edged morphology when maintained in culture, while islets exposed to stress tend to adopt a more ruffled surface.<sup>[24]</sup> To quantitatively assess changes in morphology, the circularity of individual islets was measured from light micrographs using an algorithm from ImageJ image processing software (Figure 3c–e). Circularity, a geometrical ratio defined by Equation (1), approaches 1.0 for perfect circles with smooth edges and decreases toward 0.0 when edge abrasions or defects increase perimeter but not area.

$$Circularity = \frac{4\pi \times Area}{perimeter^2} \quad (1)$$

Autocoating did not cause a significant reduction in circularity relative to uncoated islets (Figure 3f, p=0.7). Mean circularity of autocoated islets (n=88) was slightly higher than that of manually coated islets (0.570 vs. 0.531), but this difference was not statistically significant (p=0.07). Circularity analysis, like the viability analysis described above, was sufficiently sensitive to detect a significant difference between centrifuged islets (n= 30, Circularity = 0.301) and islets that had not been manipulated (n= 53, Circularity = 0.578; p=1.2 × 10<sup>-16</sup>).

Islet function was assessed using an established glucose stimulation protocol and quantitative insulin detection via ELISA. Insulin secretion did not differ significantly between autoc coated and uncoated islets in either basal ( $p=0.6$ ) or high ( $p=0.7$ ) glucose solutions (Figure 3g). The stimulation index, the ratio of insulin secretion in high versus low glucose conditions, was not significantly different between autoc coated (5.93) and uncoated (5.28) islets ( $p=0.95$ ).

In summary, we present an automated filtration and wash strategy to assemble LbL nanothin films on isolated pancreatic islets. This approach affords high quality films in a manner that is sufficiently gentle to maintain high islet viability, function, and structural integrity while reducing the likelihood of user error. Central to this effort was the adaptation of machine vision technology to sub-milliliter volume fluid measurements that created a closed feedback loop in the automated system. This report builds on our previous work describing a new class of PEM films that can be assembled on viable cells and tissues. This represents the first report of fully automated assembly of PEM films on viable cell aggregates, and represents an important step towards realizing the potential of PEMs as a cell surface engineering strategy through process automation. Knowledge gained from this study may also prove useful for processing of single cells and micron-scale particles in a controlled, high throughput manner without the need for centrifugation or manual filtration.

## Experimental Section

Experimental information is available in Supplementary Information, available from the Wiley Online Library or from the author.

## Supplementary Material

Refer to Web version on PubMed Central for supplementary material.

## Acknowledgments

This work was funded by NIH grant DK069275 (E.L. Chaikof)

## References

1. Daneman D. *Lancet*. 2006; 367:847–58. [PubMed: 16530579]
2. Karvonen M, Viik-Kajander M, Moltchanova E, Libman I, LaPorte R, Tuomilehto J. *Diabetes Care*. 2000; 23:1516–26. [PubMed: 11023146]
3. Fiorina P, Shapiro AM, Ricordi C, Secchi A. *Am J Transplant*. 2008; 8:1990–7. [PubMed: 18828765]
4. Scharp DW, Lacy PE, Santiago JV, McCullough CS, Weide LG, Falqui L, Marchetti P, Gingerich RL, Jaffe AS, Cryer PE. *Diabetes*. 1990; 39:515–8. [PubMed: 2108071]
5. Ryan EA, Lakey JR, Rajotte RV, Korbitt GS, Kin T, Imes S, Rabinovitch A, Elliott JF, Bigam D, Kneteman NM, Warnock GL, Larsen I, Shapiro AM. *Diabetes*. 2001; 50:710–9. [PubMed: 11289033]
6. Ryan EA, Paty BW, Senior PA, Bigam D, Alfadhli E, Kneteman NM, Lakey JR, Shapiro AM. *Diabetes*. 2005; 54:2060–9. [PubMed: 15983207]
7. Shapiro AM, Ricordi C, Hering BJ, Auchincloss H, Lindblad R, Robertson RP, Secchi A, Brendel MD, Berney T, Brennan DC, Cagliero E, Alejandro R, Ryan EA, DiMercurio B, Morel P, Polonsky KS, Reems JA, Bretzel RG, Bertuzzi F, Froud T, Kandaswamy R, Sutherland DE, Eisenbarth G, Segal M, Preiksaitis J, Korbitt GS, Barton FB, Viviano L, Seyfert-Margolis V, Bluestone J, Lakey JR. *N Engl J Med*. 2006; 355:1318–30. [PubMed: 17005949]
8. Cabric S, Sanchez J, Lundgren T, Foss A, Felldin M, Källén R, Salmela K, Tibell A, Tufveson G, Larsson R, Korsgren O, Nilsson B. *Diabetes*. 2007; 56:2008–15. [PubMed: 17540953]

9. Chen H, Teramura Y, Iwata H. *J Control Release*. 2011; 150:229–34. [PubMed: 21108976]
10. Stabler CL, Sun XL, Cui W, Wilson JT, Haller CA, Chaikof EL. *Bioconjug Chem*. 2007; 18:1713–5. [PubMed: 17960873]
11. Teramura Y, Iwata H. *Bioconjug Chem*. 2008; 19:1389–95. [PubMed: 18533707]
12. Wilson JT, Chaikof EL. *J Diabetes Sci Technol*. 2008; 2:746–59. [PubMed: 19885257]
13. Wilson JT, Haller CA, Qu Z, Cui W, Urlam MK, Chaikof EL. *Acta Biomater*. 2010; 6:1895–903. [PubMed: 20102751]
14. Jang JY, Lee DY, Park SJ, Byun Y. *Biomaterials*. 2004; 25:3663–9. [PubMed: 15020141]
15. Lee DY, Park SJ, Lee S, Nam JH, Byun Y. *Tissue Eng*. 2007; 13:2133–41. [PubMed: 17516853]
16. Lee DY, Park SJ, Nam JH, Byun Y. *J Control Release*. 2006; 110:290–5. [PubMed: 16324765]
17. Lee DY, Park SJ, Nam JH, Byun Y. *Tissue Eng*. 2006; 12:615–23. [PubMed: 16579694]
18. Panza JL, Wagner WR, Rilo HL, Rao RH, Beckman EJ, Russell AJ. *Biomaterials*. 2000; 21:1155–64. [PubMed: 10817268]
19. Teramura Y, Iwata H. *Transplantation*. 2009; 88:624–30. [PubMed: 19741458]
20. Xie D, Smyth CA, Eckstein C, Bilbao G, Mays J, Eckhoff DE, Contreras JL. *Biomaterials*. 2005; 26:403–12. [PubMed: 15275814]
21. Mansouri S, Merhi Y, Winnik FM, Tabrizian M. *Biomacromolecules*. 2011; 12:585–92. [PubMed: 21306170]
22. Matsusaki M, Kadowaki K, Nakahara Y, Akashi M. *Angew Chem*. 2007; 119:4773–76. *Angew Chem Intl Ed Engl*. 2007; 46:4689–92.
23. Teramura Y, Iwata H. *Biomaterials*. 2009; 30:2270–5. [PubMed: 19201021]
24. Wilson JT, Cui W, Chaikof EL. *Nano Lett*. 2008; 8:1940–8. [PubMed: 18547122]
25. Wilson JT, Cui W, Kozlovskaya V, Kharlampieva E, Pan D, Qu Z, Krishnamurthy VR, Mets J, Kumar V, Wen J, Song Y, Tsukruk VV, Chaikof EL. *J Am Chem Soc*. 2011; 133:7054–64. [PubMed: 21491937]
26. Zhi ZL, Liu B, Jones PM, Pickup JC. *Biomacromolecules*. 2010; 11:610–6. [PubMed: 20108955]
27. Miura S, Teramura Y, Iwata H. *Biomaterials*. 2006; 27:5828–35. [PubMed: 16919725]
28. Teramura Y, Kaneda Y, Iwata H. *Biomaterials*. 2007; 28:4818–25. [PubMed: 17698188]
29. Germain M, Balaguer P, Nicolas JC, Lopez F, Esteve JP, Sukhorukov GB, Winterhalter M, Richard-Foy H, Fournier D. *Biosens Bioelectron*. 2006; 21:1566. [PubMed: 16099641]
30. Veerabadrán NG, Goli PL, Stewart-Clar SS, Lvov YM, Mills DK. *Macromol Biosci*. 2007; 7:877. [PubMed: 17599337]
31. Kadowaki K, Matsusaki M, Akashi M. *Langmuir*. 2010; 26:5670–8. [PubMed: 20055371]
32. Rajagopalan P, Shen CJ, Berthiaume F, Tilles AW, Toner M, Yarmush ML. *Tissue Eng*. 2006; 12:1553–1563. [PubMed: 16846351]
33. Caruso F, Caruso RA, Mohwald H. *Science*. 1998; 282:1111–4. [PubMed: 9804547]
34. Decher G. *Science*. 1997; 277:1232–37.
35. Hiller J, Mendelsohn JD, Rubner MF. *Nat Mater*. 2002; 1:59–63. [PubMed: 12618851]
36. Jiang C, Markutsya S, Pikus Y, Tsukruk VV. *Nat Mater*. 2004; 3:721–8. [PubMed: 15448680]
37. Krogman KC, Lowery JL, Zacharia NS, Rutledge GC, Hammond PT. *Nat Mater*. 2009; 8:512–8. [PubMed: 19377464]
38. Podsiadlo P, Kaushik AK, Arruda EM, Waas AM, Shim BS, Xu J, Nandivada H, Pumphlin BG, Lahann J, Ramamoorthy A, Kotov NA. *Science*. 2007; 318:80–3. [PubMed: 17916728]
39. Fakhru'llin RF, Lvov YM. *ACS Nano*. 2012; 6:4557–64. [PubMed: 22612633]
40. Fakhru'llin RF, Zamaleeva AI, Minullina RT, Konnova SA, Paunov VN. *Chem Soc Rev*. 2012; 41:4189–4206. [PubMed: 22509497]
41. Boudou T, Cruzier T, Ren K, Blin G, Picart C. *Adv Mater*. 2010; 22:441–67. [PubMed: 20217734]
42. Elbert DL, Hubbell JA. *Chem Biol*. 1998; 5:177–183. [PubMed: 9545428]
43. Elbert DL, Hubbell JA. *J Biomed Mat Res*. 1998; 42:55–65.



44. Kenausis GL, Voros J, Elbert DL, Huang NP, Hofer R, Ruiz-Taylor L, Textor M, Hubbell JA, Spencer ND. *J Phys Chem B*. 2000; 104:3298–3309.
45. Huang NP, Michel R, Voros J, Textor M, Hofer R, Rossi A, Elbert DL, Hubbell JA, Spencer ND. *Langmuir*. 2001; 17:489–498.
46. Wilson JT, Krishnamurthy VR, Cui W, Qu Z, Chaikof EL. *J Am Chem Soc*. 2009; 131:18228–18229. [PubMed: 19961173]
47. Krol S, del Guerra S, Grupillo M, Diaspro A, Gliozzi A, Marchetti P. *Nano Lett*. 2006; 6:1933–9. [PubMed: 16968004]
48. Cohen I, Li H, Hougland JL, Mrksich M, Nagel SR. *Science*. 2001; 292:265–7. [PubMed: 11303097]
49. Kantak C, Beyer S, Yobas L, Bansal T, Trau D. *Lab Chip*. 2011; 11:1030–5. [PubMed: 21218225]

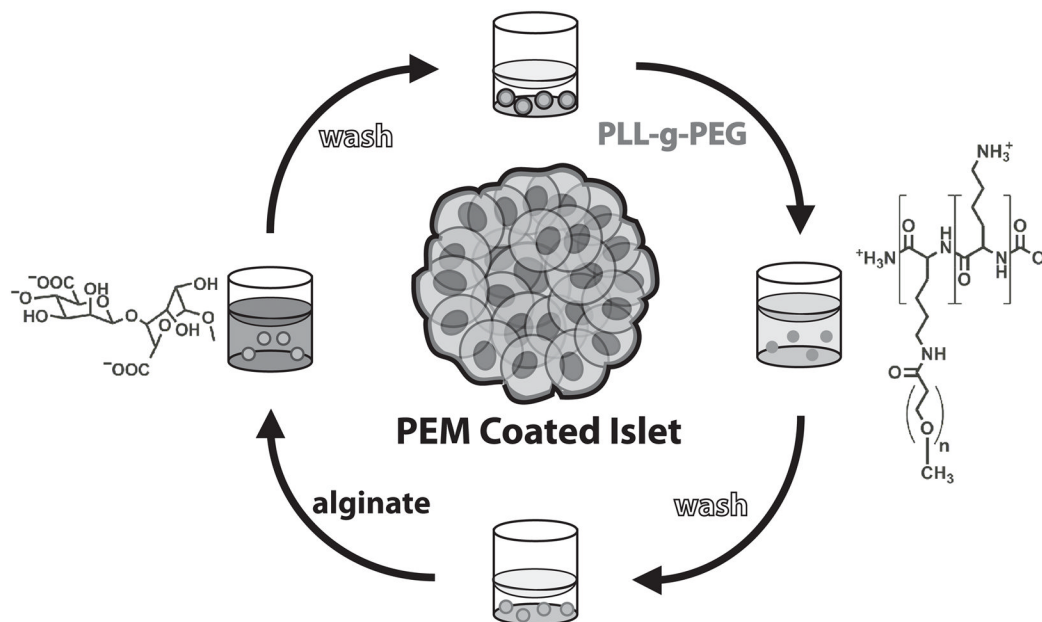


**Figure 1.** Polyelectrolyte multilayer (PEM) thin films are formed on islets by layer-by-layer (LbL) self-assembly. Islets are incubated in poly-L-lysine grafted with poly(ethylene glycol) side chains (PLL-*g*-PEG), washed with islet wash buffer three times, incubated in alginate, and washed once again with islet wash buffer three times to form each bilayer of the multilayer film.



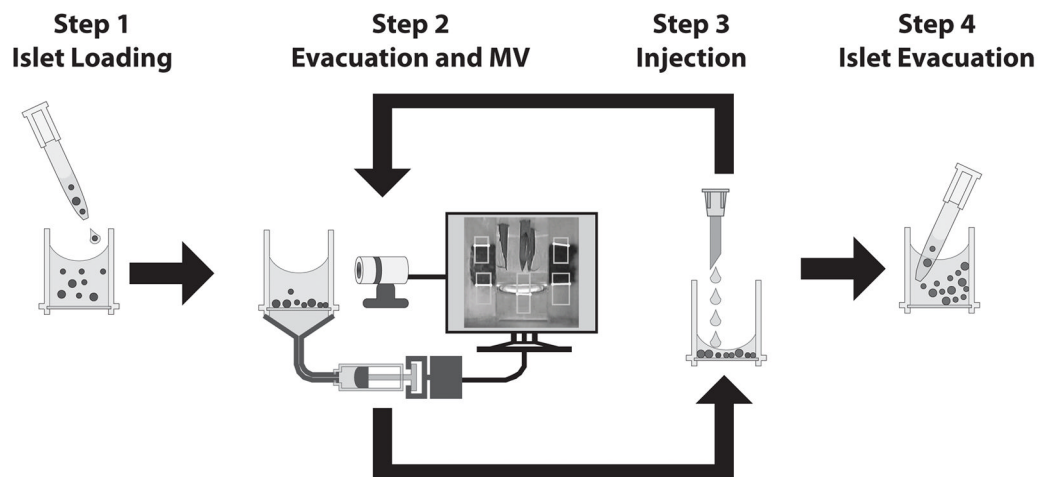


**Figure 2.**

Auto-coater process control is achieved by computer-integrated components and video feedback. **(Step 1)** Islets are injected into the reactor by hand via hand pipette. **(Step 2)** Next, solution is withdrawn through microporous mesh on the inferior surface of the reactor by an automated syringe pump. During a pause in evacuation, a webcam acquires images of the reactor and housing frame. A machine vision (MV) image analysis algorithm uses the relative locations of the fluid meniscus and fiducials (reference marks) on the reactor housing frame to calculate the volume remaining in the reactor. Evacuation time is adjusted to correct for any errors so that  $60 \pm 10 \mu\text{L}$  of solution remain in the reactor. **(Step 3)** Next, new solution is added by syringe pump. Steps 2 and 3 repeat sequentially with various wash and polyelectrolyte solutions as required for a given coating protocol. **(Step 4)** After the protocol completes, islets are withdrawn via hand pipette.

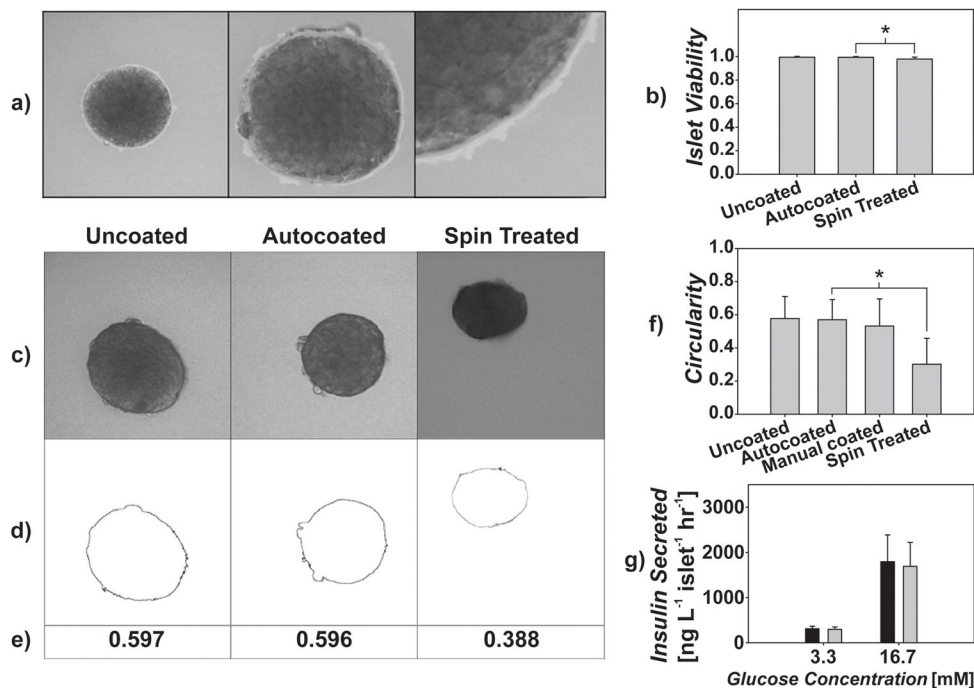


**Figure 3.**

Autocoating forms conformal PEM thin films on islets while maintaining viability, morphology, and function. a) PEM films appear uniform and without major defects after 8 bilayers of automated coating. b) Both uncoated and autocoated islets had mean viability of 99.3% ( $p=0.7$ ). Centrifugation for 15 minutes, a treatment known to induce minor damage to islets, resulted in a small but statistically significant drop in viability (to 97.9%,  $p=2.25 \times 10^{-7}$ ). c–e) To probe for changes in islet surface morphology, light micrographs (representative images, (c)) were processed with the ImageJ particle detection algorithm (d), and (e) circularity was computed for each islet. (f) Mean circularity of autocoated islets (0.570) did not differ significantly compared to uncoated islets (0.578,  $p=0.7$ ) or islets coated with the traditional manual coating method (0.532,  $p=0.7$ ), but circularity was significantly reduced in centrifuged islets (0.301,  $p=1.2 \times 10^{-16}$  vs autocoated). (g) Insulin secretion was not significantly different between uncoated and autocoated islets at either basal (3.3mM,  $p=0.6$ ) or high (16.7mM,  $p=0.7$ ) glucose concentrations. a–f)  $n=30$ –60 islets; g)  $n=60$ –100 islets per condition; \* indicates  $p<0.001$

**Table 1**

Autocoating addresses the shortcomings of manual filtration while retaining effectiveness.

	<b>Manual Filtration</b>	<b>Autocoating</b>
Out-of-culture time (hr)	3:00	3:00 <sup>a)</sup>
Human Time (hr)	3:30	1:30 <sup>a)</sup>
Human involvement	Complex Technical Skill	Execute Setup Protocol
Capacity (# of islets)	>500	>500
Control of evacuation	Human eye	Machine Vision <sup>b)</sup>
Post-evacuation void volume ( $\mu$ L)	70 $\pm$ 30	60 $\pm$ 10 <sup>b)</sup>
Polycation required (mg)	8	7 <sup>b)</sup>
Islet Yield	80–90%	91%
Islet Viability	>99%	>99%
Islet Circularity	>0.500	>0.500
Insulin Secretion	intact	intact

<sup>a)</sup> Autocoating does not reduce time needed to process islets out of culture, which depends largely on the kinetics of polyelectrolyte interactions. However, autocoating decreases human-time requirements since attention is needed only for setup and takedown, not supervision of the process itself.

<sup>b)</sup> The autocoating method improves evacuation precision, allowing optimization of polyelectrolyte solution concentration and volume to decrease total polycation demand. Islets are also better protected from the deleterious effects of exposure to air-water interfaces caused by over-evacuation.